

Article

Enhanced Separation Behavior of Metals from Simulated Printed Circuit Boards by Supergravity

Long Meng^{1,2}, Yudong Liu^{1,2} and Zhancheng Guo^{1,*}

¹ State Key Laboratory of Advanced Metallurgy, University of Science and Technology Beijing, 30 Xueyuan Road, Beijing 100083, China

² Institute of Process Engineering, Chinese Academy of Sciences, No. 1 Beier Tiao, Beijing 100190, China

* Correspondence: zcguo@ustb.edu.cn; Tel./Fax: +86-10-82375042

Abstract: Printed circuit boards (PCBs) contain valuable metals, epoxy resin, and glass fiber, resulting in them being considered as attractive secondary sources of metals. Due to the complex metal compositions in PCBs, it is difficult to clarify the mechanism of metal separation behavior in the pyrometallurgical recovery process. In this paper, pure Pb, Sn and Cu were used to simulate the effects of temperature, time, particle size and shape on the reaction and separation process. With the increase of temperature and time, the thickness of the interface reaction layer was improved. Under the same temperature and time, the reaction degree of Cu with Sn was greater than that of Cu with Pb. In the separation process, reducing temperature, time and increasing Cu particle size were conducive to the separation and recovery of Pb-Sn alloy by supergravity. Under the same or similar particle size, the recovery of Pb-Sn alloy in irregular Cu particles was lower than that in regular Cu spheres. Improving the gravity coefficient benefited the recoveries of Pb and Sn. The results will provide technical guidance for the separation and recovery of Pb, Sn and Cu from real PCBs.

Keywords: printed circuit boards; supergravity; reaction process; mechanism; separation behavior



Citation: Meng, L.; Liu, Y.; Guo, Z. Enhanced Separation Behavior of Metals from Simulated Printed Circuit Boards by Supergravity. *Metals* **2022**, *12*, 1533. <https://doi.org/10.3390/met12091533>

Academic Editors: Antonije Onjia and Petros E. Tsakiridis

Received: 8 August 2022

Accepted: 12 September 2022

Published: 16 September 2022

Publisher's Note: MDPI stays neutral with regard to jurisdictional claims in published maps and institutional affiliations.



Copyright: © 2022 by the authors. Licensee MDPI, Basel, Switzerland. This article is an open access article distributed under the terms and conditions of the Creative Commons Attribution (CC BY) license (<https://creativecommons.org/licenses/by/4.0/>).

1. Introduction

In the 21st century, electronic industry has developed rapidly, more and more electrical and electronic equipment (EEEs) are applied to real life, and the replacements of EEEs are increasing rapidly. Due to the shortening of production times and increasing use of electronic products, large quantities of electronic wastes (e-wastes) are being produced [1]. In 2021, global production of e-waste was about 57 million tons, with annual growth of 2 million tons per year [2]. Since every item of e-waste has printed circuit boards (PCBs) built in, the replacements of e-wastes result in a large quantity of waste PCBs (WPCBs) which have many valuable metals such as Pb, Sn, Cu, Au, Ag, Pt, kinds of resins and glass fibers [3,4]. Generally, approximately 70% nonmetals and 30% metals are contained in WPCBs [5]. Cu, Pb and Sn are the three most abundant metals in PCBs (Cu: ~16%, PbSn solder: ~4%), and their recoveries are of economic and ecological importance for use as a secondary raw material because of the relatively high content in comparison to the earth's crust composition [6–8].

Recently, many technologies have been developed to recover Pb, Sn, and Cu, including hydrometallurgy [9–11], bioleaching [12,13], physical method [14,15], and pyrometallurgy [6]. These methods can successfully recover and recycle different metals with some notable shortcomings in some cases. Hydrometallurgy has the advantages of selectivity in obtaining metals from solution, minimal gas emissions and high recovery. However, it was a long and complicated process, leading to large amounts of waste acid liquid and sludge [16]. The bioleaching bacteria are easy to cultivate, and the process saves production cost and improves metal recovery. However, the process is hindered by the difficulty of selecting suitable bacteria, and by the long period [17]. The physical method has attracted

more and more attention because of its low operating cost, high sorting efficiency and easy operation. However, it was limited to factors such as low efficiency and high work intensity [10]. Generally, pyrometallurgy is the most commonly used method to recover valuable metals from PCBs with high energy consumption, investment and pollution [18]. However, traditional pyrometallurgy usually used smelting to melt metals into multi-metal alloys, and the subsequent refining, impurity removal and separation of metal were also needed [19,20]. It was not conducive to the separation of metals with similar properties and melting points. Due to the complex compositions of raw materials, traditional method cannot completely separate the constituent metals. However, separating metals with similar properties and melting points in PCBs step by step is the goal of efficient recovery and utilization. Our group has developed a novel method of efficiently and economically separating metals from granulated PCBs via supergravity separation [21].

Supergravity is an efficient multi-phase reaction and separation technique that uses centrifugal force to enhance phase transfer and micromixing [22]. Different melting points or densities of solid particles and liquid melts results in particles being distributed and separated gradually along the centrifugal direction under a centrifugal field [23]. The technology has been successfully applied to the enrichment of valuable elements from different slags and wastes [24–26], the fabrication of functionally graded materials [27–29], and the removal of impurities from alloys or metals [30–32]. The application of supergravity technology to the separation and recovery of metals from PCBs is also a new approach.

Generally, metals in the polymetallic rich particles of PCBs mainly present in the form of single substance and a small amount of alloy, and their components are relatively independent. Based on the phase diagram of Pb-Sn [33], the alloys of the Pb-Sn system form a single-eutectic diagram without chemical compounds, the eutectic temperature is 183 °C, and they are melted easily at the temperature above 327 °C. According to the Cu-Sn phase diagram [34], the liquidus increases with the decrease of Sn content. When Sn > 92.4 wt.%, the interface reaction of Cu-Sn system is liquid-solid reaction at the temperature above 415 °C; when Sn = 13.5–92.4 wt.%, the equilibrium state is liquid phase and solid solution with different Sn and Cu contents at 415–793 °C, which is also the main reaction zone of Cu and Sn; when Sn < 13.5 wt.%, the equilibrium state is single solid solution at 400–800 °C. Similarly, from the Cu-Pb phase diagram [35], Cu is in solid state, while Pb is in liquid state, the solubility is very low, Pb is difficult to integrate into Cu, and almost no reaction occurs at 400–800 °C. According to the metal compositions in the PCBs, the selective melting separation of Pb, Sn, and Cu can be realized via using supergravity technology by controlling the appropriate temperature. However, due to the wide variety and complex metal compositions of PCBs (other metals with less content), pure metals are used to simulate their compositions and conduct the separation process to clarify the interface reaction and separation behavior in this work. The plate, sphere and irregular shape particle of pure metals along with the effects of reaction temperature, separation time and particle size on the separation efficiency by supergravity were investigated. The results will provide technical guidance for the supergravity separation and recovery of valuable metals in real polymetallic PCBs.

2. Experiments

2.1. Materials and Methods

In this study, pure Cu, Pb, Sn, and Pb₃₇Sn₆₃ alloy (wt.%) were purchased with a purity of 99.9 wt.%. Two kinds of metal plates with smooth surface were put into the porcelain boat and placed in the horizontal tubular furnace for heating. The mixed gas of hydrogen and argon with the flow rate of 150 mL/min and gas volume ratio of 1:1 was introduced. The metal plates were cooled to room temperature under the condition of passing protective atmosphere. The effects of temperature (400–700 °C) and reaction time (0.5–6 h) on the interfacial reaction behaviors between metal plates were investigated with a tubular furnace, as shown in Figure 1.

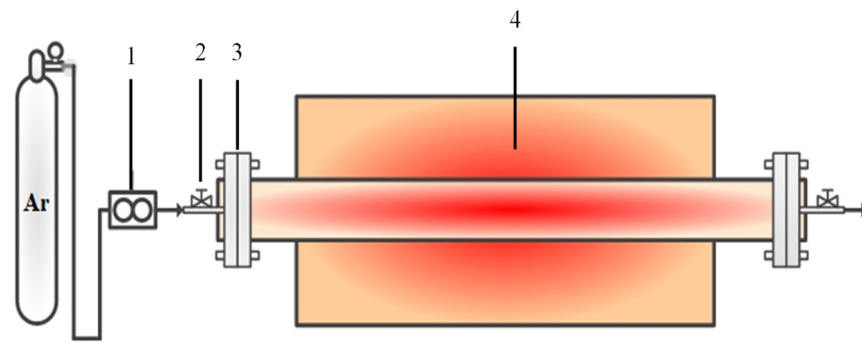


Figure 1. Experimental device flow of tubular furnace. (1. flow meter; 2. air valve; 3. flange; 4. tubular heating furnace.)

Due to the large contact area between metal plates, the metal-to-metal reaction is relatively sufficient, while in actual electronic waste, metals are mostly spherical or spheroid, it is necessary to study the interface reaction and separation behavior between metal spheres or spheroids. These experiments were carried out under the supergravity field that generated by a centrifugal apparatus with a heating furnace and a counterweight fixed symmetrically onto the horizontal rotor (Figure 2a). The centrifugal apparatus had two centrifugal tanks (Figure 2b). One was used for heating and centrifuging sample (the separation tank on the right of Figure 2b), and the other was used for balancing the equipment to keep the centrifugal process stable (the counterweight tank on the left of Figure 2b). The interfacial reaction and supergravity separation behaviors between different metal particles were studied in Figure 2. The gravity coefficient (G) was calculated as the ratio of super gravitational acceleration to normal gravitational acceleration via Equation (1):

$$G = \frac{\sqrt{g^2 + (\omega^2 R)^2}}{g} = \frac{\sqrt{g^2 + \left(\frac{N^2 R}{\pi^2 900}\right)^2}}{g} \quad (1)$$

where ω is the angular velocity (rad/s); N is the rotating speed of the centrifuge (r/min); R is the distance from the centrifugal axis to the center of the sample (m), in the experiment, $R = 0.25$ m; and g is normal gravitational acceleration.

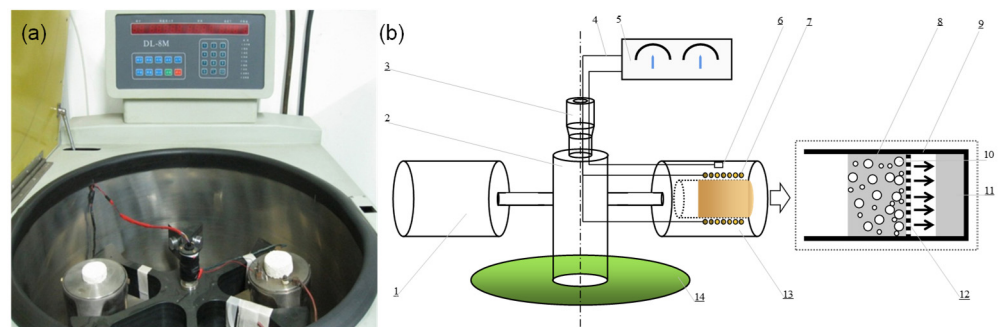


Figure 2. Photograph (a) and schematic (b) of the centrifugal separation apparatus. (1: counterweight tank; 2: centrifugal axis; 3: slip ring; 4: wire; 5: temperature controller; 6: thermocouple; 7: resistance wire; 8: Pb or Sn; 9: graphite crucible; 10: copper particle; 11: molten metal; 12: hole; 13: separation tank; 14: base).

The real WPCBs were purchased from an enterprise in China. Prior to the receipt, the PCBs were crushed, sorted, and sieved to obtain a particle size of less than 1.0 mm, a small number of nonmetallic components was retained in the enriched PCB particles, and the majority of nonmetallic materials were removed. Therefore, the total contents of metals were more than 80 wt.%, while the total contents of nonmetals were less than 20 wt.%.

The obtained PCBs contained a range of metals and alloys with different melting points, and the molten metals and alloys could be separated rapidly by supergravity. Based on the above enriched metal contents, 2.0 g Pb₃₇Sn₆₃ alloy particles and 8.0 g Cu particles (0.1–1.25 mm) of were mixed uniformly and placed into a set of graphite crucibles for the reaction and separation by supergravity melting separation. The bottom of the upper graphite crucible included the 1 mm small holes, through which metals in the liquid state could pass at the temperature of 400–600 °C. The graphite felt with the 3 mm thickness was laid at the bottom of the upper crucible to retain small solid particles. The graphite crucible was heated to the target temperature (400–600 °C) for some certain time (0.5–2 h). Then, the centrifugal apparatus was adjusted to the rotational speed (0–1338 r/min) to conduct separation isothermally for 10 min. Finally, the graphite crucible was taken out from the furnace and rapidly quenched in water.

2.2. Analysis and Treatment of Data

In the reaction process, all the samples were characterized by scanning electron microscope and energy disperse spectrum (SEM/EDS, MLA 250, FEI Quanta, Fremont, CA, USA). In the separation process, all the samples were characterized by metallographic microscope (Leica Microsystems, Model DM4M, Wetzlar, Germany), X-ray fluorescence analysis (XRF, XRF-1800, Shimadzu Corporation, Tokyo, Japan), inductively coupled plasma-optical emission spectroscopy (ICP-OES, Optima 7000DV, Perkin Elmer, Shelton, CT, USA), and SEM/EDS, respectively.

The recovery value (R_i) of Pb-Sn alloy was calculated by Equation (2):

$$R_i = \frac{m_i}{m_p \times \omega_i} \times 100\% \quad (2)$$

where m_i is the mass of Pb-Sn that separated from polymetallic particles (g); m_p is the mass of polymetallic particles; ω_i is the mass fraction of Pb-Sn in the polymetallic particles.

3. Results and Discussion

3.1. Interfacial Reaction between Metal Plates

3.1.1. Effect of Temperature on Interfacial Reaction between Metals

The microstructures of the interfaces between Pb, Sn or Cu at different temperatures (400–700 °C) with a holding time of 1 h were displayed in Figure 3. Based on the Pb-Sn phase diagram [33], Pb and Sn formed a single-eutectic diagram, and the reaction was sufficient and rapid at 400–700 °C. Therefore, Pb and Sn were evenly distributed and there was no obvious difference in the microstructure of Pb-Sn alloy. However, at the temperatures of 400–700 °C, the thickness of the interface layer between Pb and Cu increased slowly with the addition of temperature, while the thickness of the interface layer between Sn and Cu grew obviously. This is because it is difficult for liquid Pb and Cu to form a solid solution, the solubility is very small and there are liquid phase and Cu phase in this temperature range [35], while liquid Sn and Cu are easy to form a solid solution, indicating that the reaction between Sn and Cu was quick, and they had a certain solubility [34]. Temperature affected the formation of solid solution and high temperature promoted the diffusion process. Therefore, low temperature can delay the occurrence of interfacial reaction and help to separate Pb and Sn from polymetallic Cu-rich particles of WPCBs.

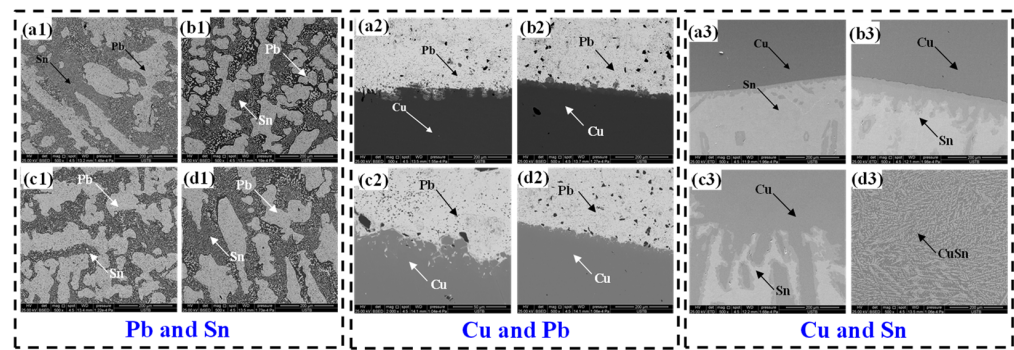


Figure 3. Microstructures of the interfaces between Pb, Sn or Cu at different temperatures. (a1–a3): 400 °C; (b1–b3): 500 °C; (c1–c3): 600 °C; (d1–d3): 700 °C.

3.1.2. Effect of Reaction Time on Interfacial Reaction between Metals

Reaction time is also an important parameter on interfacial reaction. The effects of different reaction time (0.5–6 h) on the reaction degree of Cu with Pb or Sn at 400 °C were investigated. The microstructures of the interfaces between Cu and Pb or Sn at different reaction times were displayed in Figure 4. The results indicated that the thickness of Cu–Pb interface layer did not change obviously with the addition of reaction time, while liquid metal Sn infiltrated into Cu and the Cu–Sn thickness increased significantly. These results agree well with those of Cu–Pb and Cu–Sn phase diagrams. At 400 °C, the equilibrium state of Cu–Pb system is liquid phase and Cu, while that of Cu–Sn system is liquid phase and solid solution with different Sn and Cu contents. Prolonging the reaction time is beneficial to the diffusion process of liquid Sn in Cu. In the process of separating and recovering Pb and Sn from polymetallic Cu-rich particles of WPCBs, Pb and Sn will react with Cu and reduce the recovery values of Pb and Sn. Controlling a short smelting time (holding time) is conducive to the recovery of Pb and Sn.

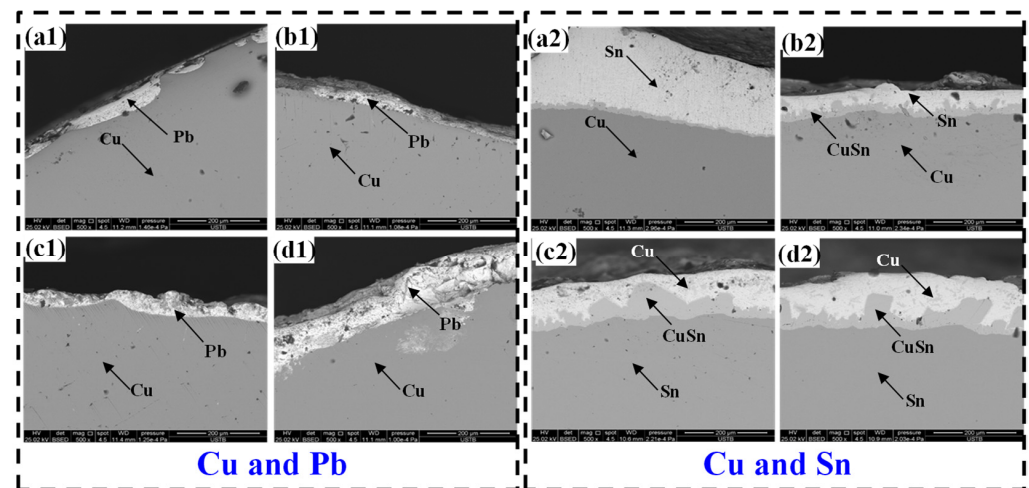


Figure 4. Microstructures of the interfaces between Cu and Pb or Sn at different times. (a1,a2): 1 h; (b1,b2): 2 h; (c1,c2): 4 h; (d1,d2): 6 h.

3.2. Interfacial Reaction and Separation Behavior between Metal Particles

3.2.1. Effects of Reaction Time and Temperature on Interfacial Reaction and Separation Behavior between Metals

In the experiments, the size of Pb–Sn alloy was 0.6 mm, and Cu particle size was 1.0 mm, the reaction times were 0.5–2 h, the rotational speed of the centrifugal apparatus was 1196 r/min ($G = 400$), and the temperature ranges were 400–600 °C. Figure 5 showed the microstructures of the interfaces between Pb–Sn alloy and Cu under different reaction times at 400 °C and 600 °C. The interfacial thickness increased with the addition of reaction

time and temperature, and the recovery rates of Pb-Sn alloy also reflected the results (as shown in Figure 6). At the same temperature, the recovery rates of Pb-Sn alloy decreased with the addition of reaction time; at the same time, the recovery rates of Pb-Sn alloy decreased as the temperature rising from 400 °C to 600 °C. PbSn and Cu reacted sufficiently and PbSn were uniformly distributed in the Cu at 600 °C. Pb-Sn alloy was consumed with Cu at high temperature in the reaction process, which was not conducive to the separation and recovery of Pb and Sn. Reducing the interface reaction and degree can improve the metal recovery rates in WPCBs. Therefore, the reasonable reaction time was 0.5 h, the temperature was 400 °C, and the recovery rate of Pb-Sn ally was 96.19%.

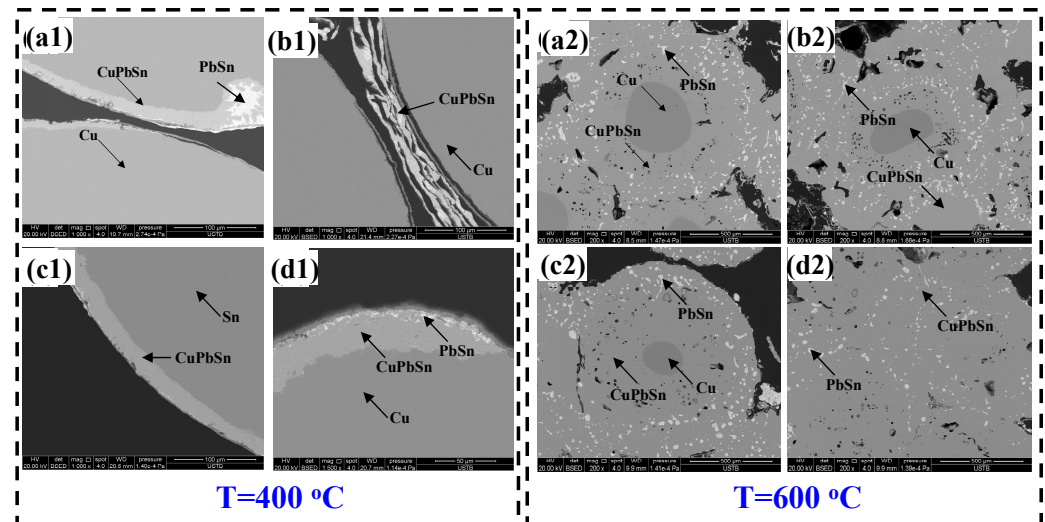


Figure 5. Microstructures of the interfaces between Pb-Sn alloy and Cu at different time and temperature. (a1,a2): 0.5 h; (b1,b2): 1 h; (c1,c2): 1.5 h; (d1,d2): 2 h.

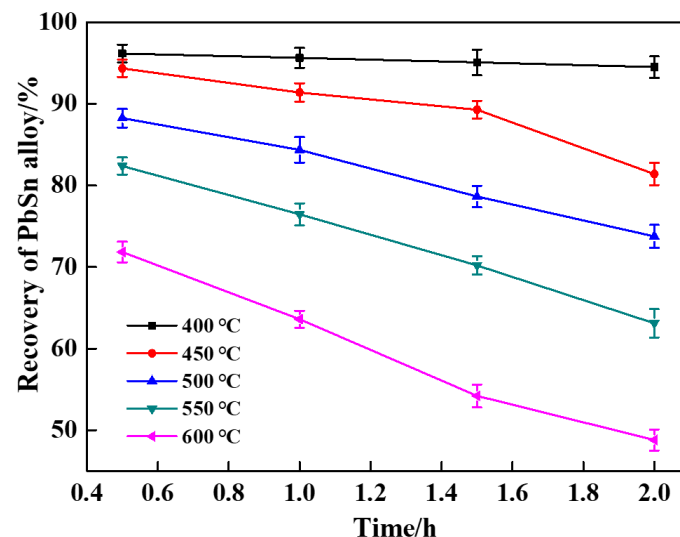


Figure 6. Effects of reaction time and temperature on recovery rate of Pb-Sn alloy.

3.2.2. Effect of Regular Cu Particle Size on Interfacial Reaction and Separation Behavior between Metals

Particle size is an important parameter affecting interfacial reaction and separation behavior. In the experiments, the size of Pb-Sn alloy was 0.6 mm, the rotational speed of the centrifugal apparatus was 1196 r/min ($G = 400$), the reaction time was 0.5 h, the temperature was 400 °C, the separation time was 10 min, and the effects of particle size of regular Cu with Pb-Sn alloy on the reaction and separation were investigated. Figure 7 was

the metallographic diagrams of Cu and Pb-Sn alloy with different Cu particle sizes after centrifugation. As indicated, the residual amount of Pb-Sn alloy in the Cu sphere decreased with the gradual increase of Cu particle size. Figure 8 displayed the effect of regular Cu sphere size on the recovery rate of Pb-Sn alloy. The results exhibited that Cu sphere size varied from 0.12 to 1.25 mm, and the recovery rates of Pb-Sn alloy increased from 28.41% to 97.73%. Large Cu particle was propitious to the separation and recovery of molten Pb-Sn alloy.

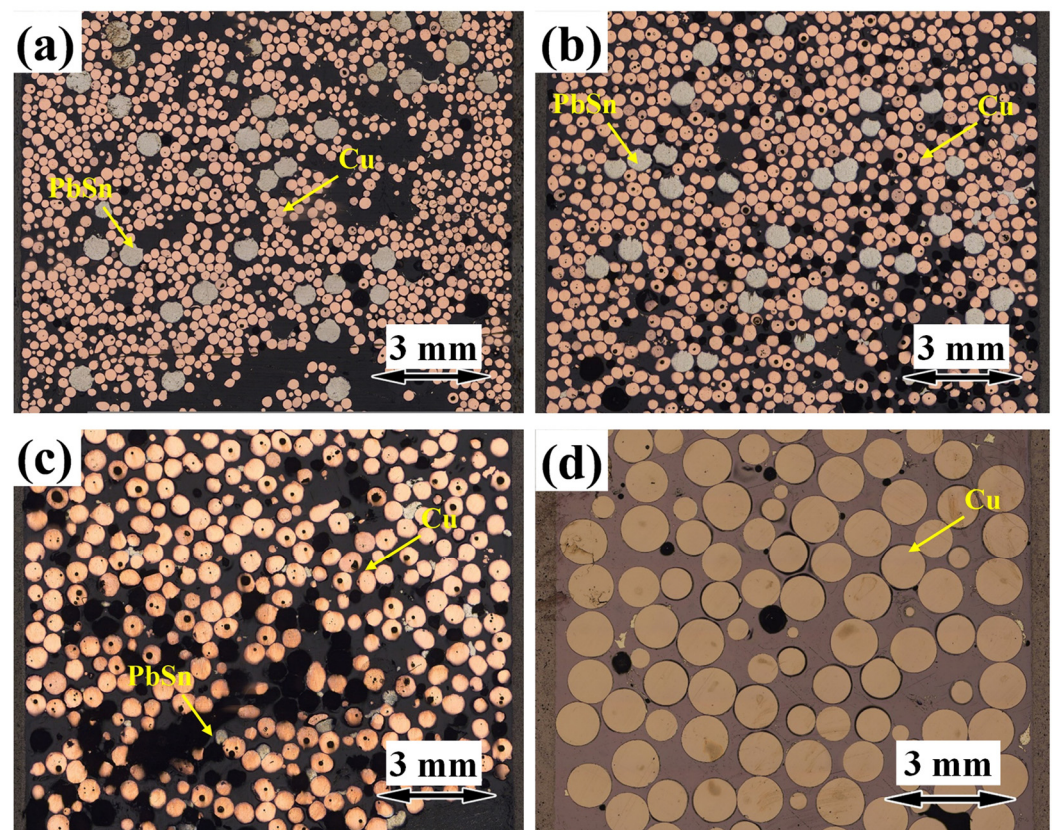


Figure 7. Metallographic diagrams of Cu and Pb-Sn alloy with different Cu particle sizes after centrifugation. (a): 0.12 mm; (b): 0.3 mm; (c): 0.5 mm; (d) 1.25 mm.

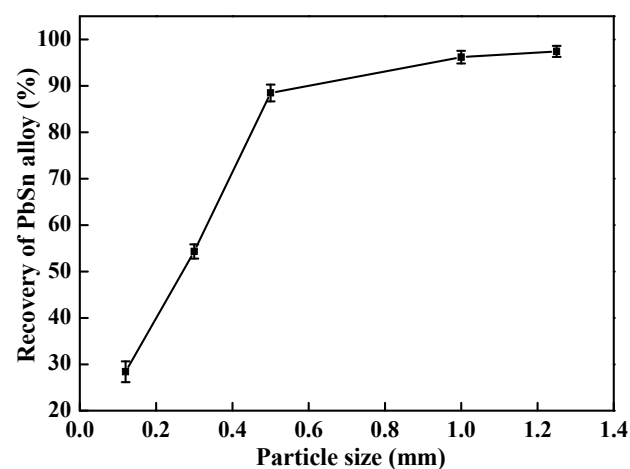


Figure 8. Effect of regular Cu particle size on the recovery rate of Pb-Sn alloy.

At 400 °C, Pb-Sn alloy is in melting state, while Cu is still in solid particle. Under normal gravity condition, due to the good wettability between metals, the liquid metals were

distributed in discontinuous droplets in the Cu particle layer, and the gravity of droplets was not enough to overcome the surface tension which was the maximum resistance of liquid metals through Cu particles. The molten droplets (Pb-Sn alloy) were not successfully separated from solid Cu particle layers, but suspended in a channel of solid metal layers, and the “retention phenomenon” was formed. This present system was approximated as an ideal model, and the tiny gap between solid particles was approximated as a capillary. The pressure (P_s) of surface tension was expressed in Equation (3):

$$P_s = \frac{2\sigma}{r'} \quad (3)$$

where σ is the Pb-Sn alloy surface tension (N/m); r' is the curvature radius (m). The gap between large particles was wide, and the molten Pb-Sn that did not participate in the reaction was easy to separate from Cu spheres.

Centrifugal force can generate centrifugal pressure on the particles to overcome surface tension and separate liquid metals from solid particles. In order to study the effect of centrifugal pressure on the behavior of mixed particles, the radial pressure (P_r) distribution at r position is expressed in Equation (4):

$$P_r = \int_{r_0}^r \rho r \omega^2 dr = \frac{1}{2} \rho (r^2 - r_0^2) \omega^2 \quad (4)$$

where r_0 is the minimum distance from the centrifugal axis to the centre of sample (m); r is the distance from the centrifugal axis to the centre of sample (m); ρ is the metallic density (kg/m^3); ω is the angular velocity (rad/s). The centrifugal pressure is proportional to the metallic density, rotational angular velocity, and square of rotating radius, respectively. Under this condition, the efficient and rapid separation of molten Pb-Sn alloy was realized by increasing the rotating speed.

3.2.3. Effect of Irregular Cu Particle Size on the Interfacial Reaction and Separation Behavior between Metals

The reaction and separation between regular spheres is an ideal process. However, most of actual e-waste particles present irregular shapes. Therefore, simulating the interface process between irregular metals truly reflected the reaction and separation behavior between e-waste particles. The particle size of Pb-Sn alloy was 0.6 mm, the rotational speed of centrifugal apparatus was 1196 r/min ($G = 400$), the reaction time was 0.5 h, the temperature was 400 °C, the separation time was 10 min, and the effects of irregular Cu sizes (0.1–1.25 mm) on the recovery of Pb-Sn alloy were systematically investigated. The metallographic diagrams of Cu and Pb-Sn alloy with different irregular Cu particle sizes after centrifugation were given in Figure 9. It can be seen that with the gradual increase of irregular Cu particle size, the residual amount of Pb-Sn alloy in Cu particle decreased, and the maximum recovery rate of Pb-Sn increased to 78.07% under the size of 1.0–1.25 mm (as shown in Figure 10). Under the same or similar Cu particle size, the recovery values of Pb-Sn alloy in irregular Cu particles were lower than those in regular Cu spheres (as shown in Figures 7 and 8). The irregular Cu was in concave convex shape, which can block the filtration and separation of molten Pb-Sn alloy. Therefore, metal particles with small and irregular particle size were not conducive to the separation and recovery of molten metals. In the actual e-waste, the vast majority of metal particles are in irregular shape, and the shape and size will have a great impact on the separation and recovery of metals.

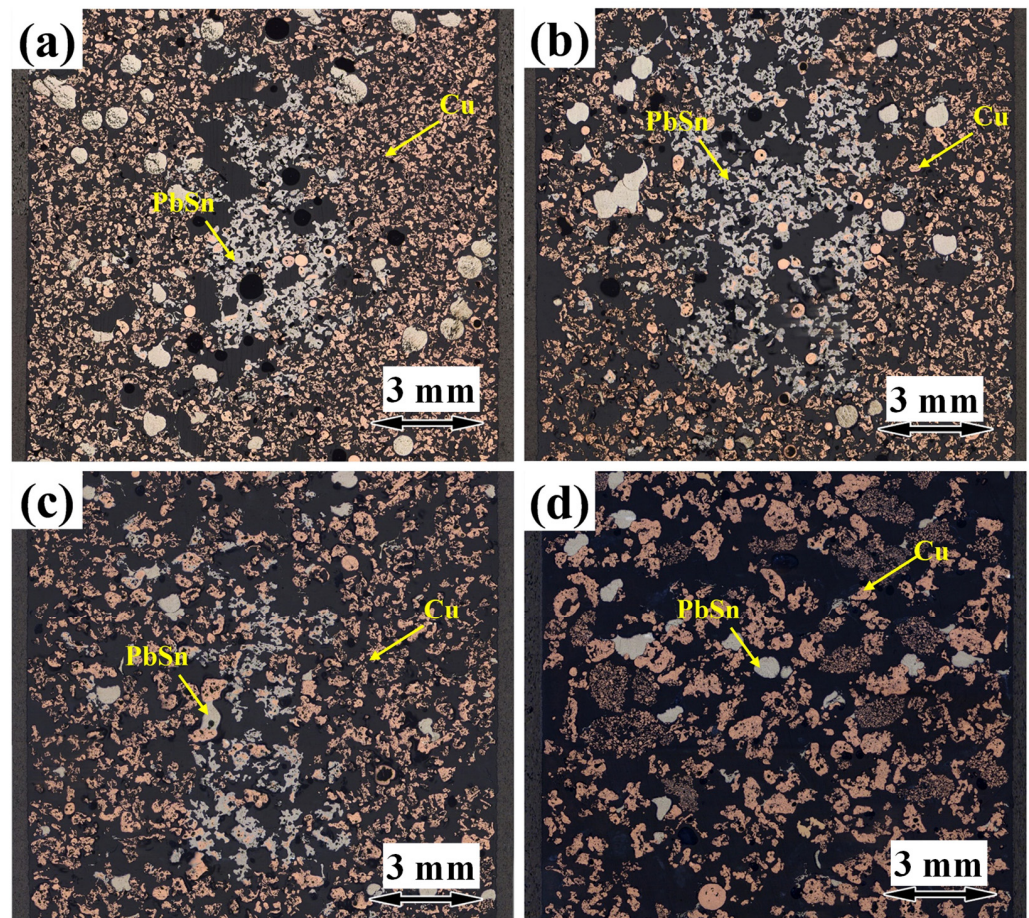


Figure 9. Metallographic diagrams of Cu and Pb-Sn alloy with different irregular Cu particle sizes after reaction and separation. (a): 0.1–0.12 mm; (b): 0.3–0.4 mm; (c): 0.4–0.5 mm; (d): 1.0–1.25 mm.

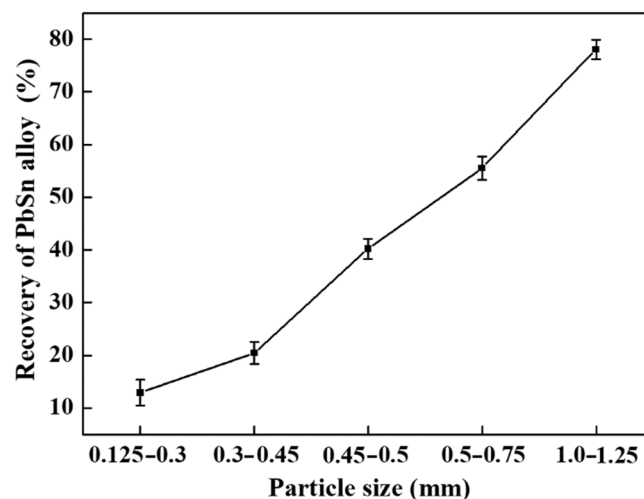


Figure 10. Effect of particle size of irregular Cu on the recovery rate of Pb-Sn alloy.

3.2.4. Effect of Gravity Coefficient on the Interfacial Reaction and Separation Behavior between Metals

The particle sizes of Pb-Sn alloy and irregular Cu were 0.6 mm and 1.0–1.25 mm, respectively, the reaction time was 0.5 h, the temperature was 400 °C, the separation time was 10 min, and the effects of gravity coefficient (1–500) on the recovery of Pb-Sn alloy were investigated in Figure 11. As indicated, the recovery rates of Pb-Sn alloy increased

from 0 to 82.23% with the gravity coefficient varying from 1 to 500. Compared to normal gravity separation ($G = 1$), supergravity separation separated Pb-Sn alloy quickly. When the $G > 50$, the centrifugal pressure (P_r) was much greater than the additional pressure (P_s) (namely $P_r \gg P_s$), the centrifugal acceleration of Pb-Sn droplets was huge, the movement was very fast, and the time was very short. When the gravity coefficient transcended 200, the increasing trend of recovery rate of Pb-Sn alloy slowed down, indicating that the molten alloy had good fluidity, and super gravity greatly improved its recovery rate. Therefore, supergravity technology has the advantage of high efficiency.

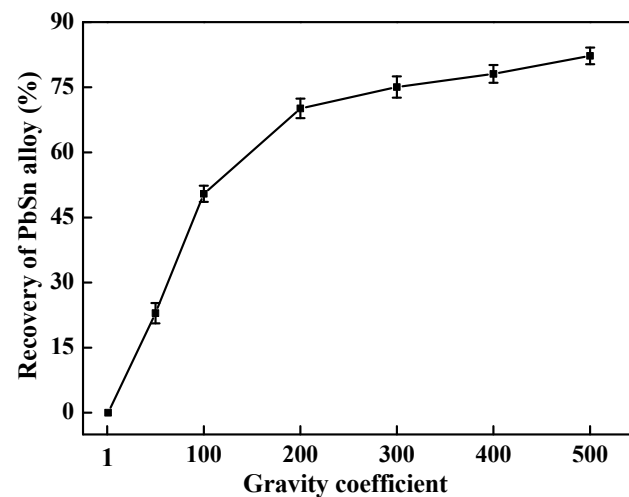


Figure 11. Effect of gravity coefficient on the recovery rate of Pb-Sn alloy.

The goal of efficient recycling of PCBs is to separate metals in the form of single substance. However, chemical reaction will inevitably occur to form alloys with different melting points in the pyrometallurgical process. It is difficult to completely separate the metals in the form of single element. Therefore, supergravity selective melting separation of metals with similar melting points is an effective recovery method. The obtained alloys are used as industrial raw materials in different industrial fields, which not only recycle waste resources, but also realize environmental protection. Future studies will examine the selective separation from complex electronic waste, and the potential of the proposed process to scale-up, to evaluate the possibility of its application on an industrial scale.

4. Conclusions

In this paper, by simulating the interfacial reaction and separation process between pure Pb, Sn, or Cu, the complex reaction behavior of polymetallic in PCBs was mastered. Based on the principle of phase diagrams and reasonable composition design, the separation between metals is strengthened by adjusting temperature and time and applying supergravity, which is beneficial to reduce the reaction degree between metals and increase the recovery rate of metals. In the metal reaction process, the thickness of interfacial reaction layer was improved by increasing temperature and time. When the temperature was above 400 °C, Pb and Sn were easy to form alloy phase. Under the same temperature and time, the reaction degree of Cu-Sn was greater than that of Cu-Pb. Reducing reaction time and temperature was conducive to reducing the reaction degree and separating metals. Supergravity selective melting separation of metals is an effective recovery method. With the increase of Cu particle size, the recovery of Pb-Sn alloy increased gradually. Under the same or similar Cu size, the recoveries of Pb-Sn alloy in irregular Cu particles were lower than those in regular Cu spheres. Under Cu particle size of 1.25 μm and gravity coefficient of 400, the recovery rates of Pb-Sn alloy were 97.73% in regular shape and 78.07% in irregular shape at 400 °C for 0.5 h, respectively. Increasing the gravity coefficient was beneficial to the recovery of Pb-Sn alloy, and the recovery value was 82.23% under the gravity coefficient of 500 at 400 °C. This process provides technical guidance for the efficient

separation and recovery of Pb, Sn and Cu from real PCBs and improves the economic and environmental benefits of metal recovery process. More detailed investigations are required to further evaluate this separation process with the real electronic wastes.

Author Contributions: Conceptualization, L.M.; methodology, L.M.; investigation, L.M.; writing—original draft preparation L.M.; writing assistance, Y.L.; deriving the theoretical framework, Z.G.; supervision, Z.G.; design guide, Z.G. All authors have read and agreed to the published version of the manuscript.

Funding: This work was supported by the National Natural Science Foundation of China (Grant No. 52004264), China Postdoctoral Science Foundation (Grant No. 2022M711989), the National Key R&D Program of China (Grant No. 2021YFC1910502) and the Key Research Program of the Chinese Academy of Sciences (Grant No. ZDRW-CN-2020-1).

Institutional Review Board Statement: Not applicable.

Informed Consent Statement: Not applicable.

Data Availability Statement: Not applicable.

Conflicts of Interest: The authors declare no conflict of interest.

References

1. Calgaro, C.O.; Schlemmer, D.F.; Da, S.M.; Maziero, E.V.; Tanabe, E.H.; Bertuol, D.A. Fast copper extraction from printed circuit boards using supercritical carbon dioxide. *Waste Manag.* **2015**, *45*, 289–297. [[CrossRef](#)] [[PubMed](#)]
2. Cheng, Z.P.; Shi, Q.Y.; Wang, Y.; Zhao, L.C.; Li, X.X.; Sun, Z.Y.; Lu, Y.; Liu, N.; Su, G.Y.; Wang, L.; et al. Electronic Waste Driven Pollution of Liquid Crystal Monomers: Environmental Occurrence and Human Exposure in Recycling Industrial Parks. *Environ. Sci. Technol.* **2022**, *56*, 2248–2257. [[CrossRef](#)]
3. Choubey, P.K.; Panda, R.; Jha, M.K.; Lee, J.C.; Pathak, D.D. Recovery of copper and recycling of acid from the leach liquor of discarded Printed Circuit Boards (PCBs). *Sep. Purif. Technol.* **2015**, *156*, 269–275. [[CrossRef](#)]
4. Jha, M.K.; Kumari, A.; Choubey, P.K.; Lee, J.C.; Kumar, V.; Jeong, J. Leaching of lead from solder material of waste printed circuit boards (PCBs). *Hydrometallurgy* **2012**, *121*, 28–34. [[CrossRef](#)]
5. Huang, K.; Guo, J.; Xu, Z. Recycling of waste printed circuit boards: A review of current technologies and treatment status in China. *J. Hazard. Mater.* **2009**, *164*, 399–408. [[CrossRef](#)] [[PubMed](#)]
6. Zhan, L.; Xu, Z.M. Separating and Recovering Pb from Copper-Rich Particles of Crushed Waste Printed Circuit Boards by Evaporation and Condensation. *Environ. Sci. Technol.* **2011**, *45*, 5359–5365. [[CrossRef](#)] [[PubMed](#)]
7. Cayumil, R.; Khanna, R.; Rajarao, R.; Mukherjee, P.S.; Sahajwalla, V. Concentration of precious metals during their recovery from electronic waste. *Waste Manag.* **2016**, *57*, 121–130. [[CrossRef](#)]
8. Veit, H.M.; Diehl, T.R.; Salami, A.P.; Rodrigues, J.S.; Bernardes, A.M.; Tenório, J.A. Utilization of magnetic and electrostatic separation in the recycling of printed circuit boards scrap. *Waste Manag.* **2005**, *25*, 67–74. [[CrossRef](#)]
9. Park, Y.J.; Fray, D.J. Recovery of high purity precious metals from printed circuit boards. *J. Hazard. Mater.* **2009**, *164*, 1152–1158. [[CrossRef](#)]
10. Kumari, A.; Jha, M.K.; Lee, J.C.; Singh, R.P. Clean process for recovery of metals and recycling of acid from the leach liquor of PCBs. *J. Clean Prod.* **2016**, *112*, 4826–4834. [[CrossRef](#)]
11. Alzate, A.; López, M.E.; Serna, C. Recovery of gold from waste electrical and electronic equipment (WEEE) using ammonium persulfate. *Waste Manag.* **2016**, *57*, 113–120. [[CrossRef](#)] [[PubMed](#)]
12. Yang, T.; Xu, Z.; Wen, J.; Yang, L. Factors influencing bioleaching copper from waste printed circuit boards by *Acidithiobacillus ferrooxidans*. *Hydrometallurgy* **2009**, *97*, 29–32. [[CrossRef](#)]
13. Yang, Y.; Chen, S.; Li, S.; Chen, M.; Chen, H.; Liu, B. Bioleaching waste printed circuit boards by *Acidithiobacillus ferrooxidans* and its kinetics aspect. *J. Biotechnol.* **2014**, *173*, 24–30. [[CrossRef](#)] [[PubMed](#)]
14. Eswaraiah, C.; Kavitha, T.; Vidyasagar, S.; Narayanan, S.S. Classification of metals and plastics from printed circuit boards (PCB) using air classifier. *Chem. Eng. Prog.* **2008**, *47*, 565–576. [[CrossRef](#)]
15. Jiang, W.; Jia, L.; Zhen-Ming, X. A new two-roll electrostatic separator for recycling of metals and nonmetals from waste printed circuit board. *J. Hazard. Mater.* **2009**, *161*, 257–262. [[CrossRef](#)] [[PubMed](#)]
16. Long, L.; Sun, S.; Zhong, S.; Dai, W.; Liu, J.; Song, W. Using vacuum pyrolysis and mechanical processing for recycling waste printed circuit boards. *J. Hazard. Mater.* **2010**, *177*, 626–632. [[CrossRef](#)]
17. Wang, L.; Li, Q.; Li, Y.; Sun, X.; Li, J.; Shen, J.; Han, W.; Wang, L. A novel approach for recovery of metals from waste printed circuit boards and simultaneous removal of iron from steel pickling waste liquor by two-step hydrometallurgical method. *Waste Manag.* **2018**, *71*, 411–419. [[CrossRef](#)]
18. Fogarasi, S.; Imre-Lucaci, F.; Imre-Lucaci, Á.; Ilea, P. Copper recovery and gold enrichment from waste printed circuit boards by mediated electrochemical oxidation. *J. Hazard. Mater.* **2014**, *273*, 215–221. [[CrossRef](#)]

19. Zhou, Y.; Qiu, K. A new technology for recycling materials from waste printed circuit boards. *J. Hazard. Mater.* **2010**, *175*, 823–828. [[CrossRef](#)]
20. Bidini, G.; Fantozzi, F.; Bartocci, P.; D'Alessandro, B.; D'Amico, M.; Laranci, P.; Scozza, E.; Zagaroli, M. Recovery of precious metals from scrap printed circuit boards through pyrolysis. *J. Anal. Appl. Pyrol.* **2015**, *111*, 140–147. [[CrossRef](#)]
21. Feng, P.; Wang, Z.; Meng, L.; Guo, Z.C. Supergravity-enhanced liquation crystallization for metal recovery from waste printed circuit boards. *Chem. Eng. Prog.* **2022**, *173*, 1–8. [[CrossRef](#)]
22. Zhao, L.X.; Guo, Z.C.; Wang, Z.; Wang, M.Y. Removal of low content impurities from Al by super-gravity. *Metall. Mater. Trans. B* **2010**, *41*, 505–508. [[CrossRef](#)]
23. Meng, L.; Wang, Z.; Guo, Z. Effective separation of fusing agent from refined magnesium slag by supergravity technology. *Chem. Eng. Process. Process Intensif.* **2022**, *175*, 108915. [[CrossRef](#)]
24. Menges, R.A.; Menges, T.S.; Bertrand, G.L.; Armstrong, D.W.; Spino, L.A. Extraction of nonionic surfactants from waste water using centrifugal partition chromatography. *J. Liq. Chromatogr. Relat. Technol.* **2012**, *15*, 2909–2925. [[CrossRef](#)]
25. Wang, Z.; Gao, J.; Shi, A.; Meng, L.; Guo, Z. Recovery of zinc from galvanizing dross by a method of super-gravity separation. *J. Alloys Compd.* **2018**, *735*, 1997–2006. [[CrossRef](#)]
26. Cambiella, A.; Benito, J.M.; Pazos, C.; Coca, J. Centrifugal separation efficiency in the treatment of waste emulsified oils. *Chem. Eng. Res. Des.* **2006**, *84*, 69–76. [[CrossRef](#)]
27. Rahimipour, M.R.; Sobhani, M. Evaluation of centrifugal casting process parameters for in situ fabricated functionally gradient Fe-TiC composite. *Metall. Mater. Trans. B* **2013**, *44*, 1120–1123. [[CrossRef](#)]
28. Watanabe, Y.; Kurahashi, M.; Kim, I.S.; Miyazaki, S.; Kumai, S.; Sato, A.; Tanaka, S.I. Fabrication of fiber-reinforced functionally graded materials by a centrifugal in situ method from Al-Cu-Fe ternary alloy. *Compos. Part A* **2006**, *37*, 2186–2193. [[CrossRef](#)]
29. Xie, Y.; Liu, C.; Zhai, Y.; Wang, K.; Ling, X. Centrifugal casting processes of manufacturing in situ functionally gradient composite materials of Al-19Si-5Mg alloy. *Rare Met.* **2009**, *28*, 405–411. [[CrossRef](#)]
30. Meng, L.; Wang, Z.; Wang, L.; Guo, L.; Guo, Z. Novel and efficient purification of scrap Al-Mg alloys using supergravity technology. *Waste Manag.* **2021**, *119*, 22–29. [[CrossRef](#)] [[PubMed](#)]
31. Li, J.W.; Guo, Z.C.; Li, J.C.; Yu, L.Z. Super gravity separation of purified Si from solvent refining with the Al-Si alloy system for solar grade silicon. *Silicon* **2014**, *7*, 239–246. [[CrossRef](#)]
32. Song, G.; Song, B.; Yang, Z.; Yang, Y.; Zhang, J. Removal of inclusions from molten aluminum by supergravity filtration. *Metall. Mater. Trans. B* **2016**, *47*, 3435–3445. [[CrossRef](#)]
33. Zeng, X.; Li, J.; Xie, H.; Liu, L. A novel dismantling process of waste printed circuit boards using water-soluble ionic liquid. *Chemosphere* **2013**, *93*, 1288–1294. [[CrossRef](#)] [[PubMed](#)]
34. Havlik, T.; Orac, D.; Petranikova, M.; Miskufova, A.; Kukurugya, F.; Takacova, Z. Leaching of copper and tin from used printed circuit boards after thermal treatment. *J. Hazard. Mater.* **2010**, *183*, 866–873. [[CrossRef](#)]
35. Zhang, C.; Jiang, W.; Yang, B.; Liu, D.; Xu, B.; Yang, H. Experimental investigation and calculation of vapor–liquid equilibria for Cu–Pb binary alloy in vacuum distillation. *Fluid Phase Equilib.* **2015**, *405*, 68–72. [[CrossRef](#)]